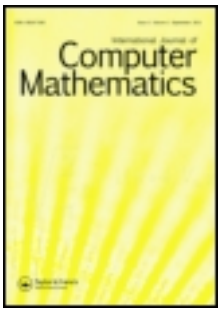

International Journal of Computer Mathematics

Publication details, including instructions for authors and subscription information:
http://www.tandfonline.com/loi/gcom20

A meshless approximate solution of mixed Volterra-Fredholm integral equations

H. Laeli Dastjerdi [a], F. M. Maalek Ghaini [a] & M. Hadizadeh [b]

[a] Department of Mathematics, Yazd University, Yazd, Iran

[b] Department of Mathematics, K.N. Toosi University of Technology, Tehran, Iran

Accepted author version posted online: 21 Aug 2012.Version of record first published: 17 Sep 2012.

To cite this article: H. Laeli Dastjerdi, F. M. Maalek Ghaini & M. Hadizadeh (2012): A meshless approximate solution of mixed Volterra-Fredholm integral equations, International Journal of Computer Mathematics, DOI:10.1080/00207160.2012.720677

To link to this article: http://dx.doi.org/10.1080/00207160.2012.720677

International Journal of Computer Mathematics
2012, 1–12, iFirst

A meshless approximate solution of mixed Volterra–Fredholm integral equations

H. Laeli Dastjerdi[a]*, F.M. Maalek Ghaini[a] and M. Hadizadeh[b]

[a]*Department of Mathematics, Yazd University, Yazd, Iran;* [b]*Department of Mathematics, K.N. Toosi University of Technology, Tehran, Iran*

(*Received 25 September 2011; revised version received 9 January 2012; second revision received 20 May 2012; third revision received 1 August 2012; fourth revision received 6 August 2012; accepted 9 August 2012*)

This paper presents a meshless method using a radial basis function collocation scheme for numerical solution of mixed Volterra–Fredholm integral equations, where the region of integration is a non-rectangular domain. We will show that this method requires only a scattered data of nodes in the domain. It is shown that the proposed scheme is simple and computationally attractive. Applications of the method are also demonstrated through illustrative examples.

Keywords: mixed Volterra–Fredholm integral equation; collocation method; radial basis functions; meshless method; numerical treatment

2010 Mathematics Subject Classifications: 45A99; 45A05

1. Introduction

The solution of the mixed Volterra–Fredholm integral equations has been a subject of considerable interest. Consider the following mixed Volterra–Fredholm integral equation

$$u(x,t) - \int_0^t \int_\Omega K(x,t,\xi,s)u(\xi,s)\,\mathrm{d}\xi\,\mathrm{d}s = f(x,t), \quad (x,t) \in \Omega \times [0,T], \tag{1}$$

where $u(x,t)$ is an unknown function, the functions $f(x,t)$ and $K(x,t,\xi,s)$ are continuous on $\Omega \times [0,T]$ and $C((\Omega \times [0,T])^2)$, respectively, and Ω is a compact subset of $\mathbb{R}^n (n = 1,2,3)$, with convenient norm $\|\cdot\|$. Equation (1) can be written in the abstract form

$$u - \mathcal{T}u = f,$$

where the integral operator $\mathcal{T} : C(\Omega \times [0,T]) \to C(\Omega \times [0,T])$ is defined as

$$(\mathcal{T}u)(x,t) = \int_0^t \int_\Omega K(x,t,\xi,s)u(\xi,s)\,\mathrm{d}\xi\,\mathrm{d}s.$$

*Corresponding author. Email: hojatlaeli@stu.yazduni.ac.ir

ISSN 0020-7160 print/ISSN 1029-0265 online

http://dx.doi.org/10.1080/00207160.2012.720677
http://www.tandfonline.com

Throughout the paper, we suppose that $f \in C(\Omega \times [0,T]), K \in C((\Omega \times [0,T])^2)$, and then Equation (1) possesses a unique solution (see e.g. [4,13,16] for further details).

This type of equations arises in the theory of parabolic boundary value problems, the mathematical modelling of the spatio-temporal development of epidemic models, and various physical and biological problems. Detailed descriptions and analysis of these models may be found in [5,19].

As far as we know, there are no numerical based methods for Equation (1) with dim $\Omega \geq 2$. So, in this paper, we assume Ω is a bounded two-dimensional region. Actually, few numerical methods for solving Equation (1) are known when Ω is a subset of $\mathbb{R}$. Some projection methods for numerical treatment of Equation (1) are given in [10,11,13]. Kauthen [13] studied continuous time collocation and time discretization collocation methods, and analysed their global discrete convergence properties as well as local and global superconvergence. The results of Kauthen have been extended to nonlinear Volterra–Fredholm integral equations by Brunner [3]. Guoqiang [9] considered the particular trapezoidal Nystrom method for Equation (1) and gave its asymptotic error expansion. Maleknejad and Hadizadeh [14] and Wazwaz [20] used a technique based on the Adomian decomposition method for the solution of Equation (1). Moreover, Banifatemi *et al.* [1] applied two-dimensional Legendre wavelets method to mixed Volterra–Fredholm integral equations. Recently, Yildirim [21] applied homotopy perturbation method for Equation (1).

For solving Equation (1) on a non-rectangular region, the domain must be segmented to small triangles and numerical integration over the segments is needed. Triangulations and mesh refinement are major difficulties in these methods. So, by using the meshless methods, we may overcome these problems. In recent years, meshless techniques have attracted the attention of researchers. In a meshless method, a set of scattered nodes is used instead of meshing the domain of the problem. Some well-known meshless schemes have been considered by the authors, for instance, moving least-square method [22], element-free Galerkin method [2], boundary node method [15], etc.

In this paper, we will use the radial basis function (RBFs) approximation for numerical solution of mixed Volterra–Fredholm integral equations where Ω is a non-rectangular region. The remainder of the paper is organized as follows: in Section 2, we give a brief survey of RBFs. In Section 3, the proposed method is introduced and applied on Equation (1), and finally in Section 4, some numerical and experimental results are reported.

2. RBF approximation

RBFs were introduced in [12] and they form a primary tool for multivariate interpolation. They are also receiving increased attention for solving partial differential equations in irregular domains. An RBF depends only on the distance to a centre point x_j and is of the form $\phi(\|x - x_j\|)$. The RBF may also have a shape parameter c. This parameter can be chosen for controlling the shape of functions. Determination of a reasonable c is still an outstanding research problem. A good value for the shape parameter can be found using statistical methods such as cross-validation or maximum-likelihood estimation [6]. Over the last two decades, some progress has been reported

Table 1. Some well-known functions that generate RBFs.

Name of function	Definition
Gaussian (GA)	$\phi(r) = \exp(-cr^2)$
Hardy multiquadrics (MQ)	$\phi(r) = (r^2 + c^2)^{1/2}$
Inverse multiquadrics (IMQ)	$\phi(r) = (r^2 + c^2)^{-1/2}$
Inverse quadric (IQ)	$\phi(r) = (r^2 + c^2)^{-1}$

to select a usable shape parameter. For some new work on optimal choice of this parameter, we refer the interested reader to the recent papers [7,8,17]. Some of the most popular RBFs are given in Table 1.

A key feature of an RBF method is that it does not require a grid. The method works with points scattered throughout the domain of interest, and the RBF interpolant is a linear combination of RBFs centred at the scattered points x_j,

$$u(x) = \sum_{j=1}^{N} \lambda_j \phi(\|x - x_j\|), \tag{2}$$

where the coefficient λ_j is usually determined by collocation with given discrete data, such as function values. Collocating of x_j in Equation (2) leads us to the following symmetric linear system:

$$A\Lambda = U,$$

where

$$U = [u(x_1), u(x_2), \ldots, u(x_N)],$$

and the entries of the matrix A and Λ are given by

$$a_{kj} = \phi(\|x_k - x_j\|), \quad \Lambda = [\lambda_1, \lambda_2, \ldots, \lambda_N]^{\mathrm{T}}, \quad k,j = 1, \ldots, N.$$

The matrix A can be shown to be positive definite and therefore non-singular for distinct interpolation points for GA, IMQ and IQ by Schoenberg's theorem [18]. Although the matrix A is non-singular in the above cases, usually it is very ill-conditioned. Therefore, a small perturbation in initial data may produce large amount of perturbation in the solution. Using a suitable method such as truncated singular value decomposition (TSVD) method and more precision arithmetic in computations, we can overcome this difficulty.

In what follows, we consider some definitions for the convergence on native space [6].

DEFINITION 1 (See [6]) *The fill distance of a given set $\mathcal{X} = \{x_1, \ldots, x_n\}$ consisting of pairwise distinct points in Ω can be defined as*

$$h_{\mathcal{X},\Omega} = \sup_{x \in \Omega} \min_{x_j \in \mathcal{X}} \|x - x_j\|,$$

which indicates how well the data in the set $\mathcal{X}$ fill out the domain Ω.

DEFINITION 2 (See [6]) *The definition of the native space is*

$$\mathcal{N}_\phi = \left\{ f \in L_2(\mathbb{R}^s) \cap C(\mathbb{R}^s) : \frac{\hat{f}}{\sqrt{\hat{\phi}}} \in L_2(\mathbb{R}^s) \right\},$$

where $\hat{\phi}$ is a Fourier transform of ϕ.

THEOREM (See [6]) *Let $\Omega \subseteq \mathbb{R}^2$ and suppose that the points $\mathcal{X} = \{x_1, \ldots, x_n\}$ are distinct. Denote the interpolate to $u \in \mathcal{N}_\phi$ by u_n. Then, there is a positive constant C such that for every $x \in \Omega$ and for GA RBF, we have*

$$\|u - u_n\|_{L_\infty(\Omega)} \leq \exp\left(\frac{-C |\log h_{\mathcal{X},\Omega}|}{h_{\mathcal{X},\Omega}} \right) \|u\|_{\mathcal{N}_\phi}.$$

3. The proposed method

Suppose $0 = t_0 < t_1 < \cdots < t_M = T$ be a scattered set of data in $[0, T]$ and $x_0, x_1, \ldots, x_N$ be a scattered set of nodes in Ω. We assume that Ω has a non-rectangular shape. In the sequel, we consider the following three cases for Ω:

(1) *A domain of the first kind*:

$$\Omega = \{(\sigma, \tau) \in \mathbb{R}^2 : a \le \tau \le b, v_1(\tau) \le \sigma \le v_2(\tau)\},$$

where $v_1(\tau)$ and $v_2(\tau)$ are continuous functions of τ.

(2) *A domain of the second kind*:

$$\Omega = \{(\sigma, \tau) \in \mathbb{R}^2 : c \le \sigma \le d, v_1(\sigma) \le \tau \le v_2(\sigma)\},$$

where $v_1(\sigma)$ and $v_2(\sigma)$ are continuous functions of σ.

(3) *A domain of the third kind*: If a domain is neither of the first kind nor of the second kind but could be separated to a finite number of the first or second sub-domains, then it is called a domain of the third kind.

Here, we propose the method when Ω is a domain of the first kind. Also the second kind is similarly straightforward by commuting the order of the variables. We can separate a domain of the third kind to a finite number of sub-domains of the first or second kinds and then apply the method in each sub-domain as described earlier. For approximating the solution of Equation (1), we suppose

$$u^{M,N}(x,t) = \sum_{j=0}^{M} \sum_{k=0}^{N} c_{kj} \phi_k(x) \eta_j(t), \quad (x,t) \in \Omega \times [0,T], \tag{3}$$

as an approximate for the exact solution $u(x,t)$, where

$$\phi_k(x) = \phi(\|x - x_k\|), \quad k = 0, \ldots, N,$$
$$\eta_j(t) = \phi(|t - t_j|), \quad j = 0, \ldots, M.$$

For simplicity, we can write Equation (3) as

$$u(x,t) \approx \sum_{\mu=1}^{Q} d_\mu \psi_\mu(x,t), \quad (x,t) \in \Omega \times [0,T], \tag{4}$$

where $d_\mu = c_{kj}$, $\psi_\mu(x,t) = \phi_k(x)\eta_j(t)$ and $Q = (M+1)(N+1)$. The index μ is determined by the equation $\mu = (N+1)j + k + 1$. Now by replacing Equation (4) in Equation (1), we have

$$\sum_{\mu=1}^{Q} d_\mu \left[\psi_\mu(x,t) - \int_0^t \int_\Omega K(x,t,\xi,s) \psi_\mu(\xi,s) \, \mathrm{d}\xi \, \mathrm{d}s \right] = f(x,t), \quad (x,t) \in \Omega \times [0,T]. \tag{5}$$

Then, we convert the interval $[0,t]$ to the fixed interval $[-1,1]$ by using a simple linear transformation of the form

$$s(t,\theta) = \frac{t}{2}\theta + \frac{t}{2},$$

and so Equation (5) takes the following form:

$$\sum_{\mu=1}^{Q} d_\mu \left[\psi_\mu(x,t) - \int_{-1}^{1} \int_{\Omega} \frac{t}{2} K(x,t,\xi,s(t,\theta)) \psi_\mu(\xi, s(t,\theta)) \, \mathrm{d}\xi \, \mathrm{d}\theta \right] = f(x,t). \tag{6}$$

Without loss of generality, we assume that

$$\Omega = \{\xi = (\sigma,\tau) \in \mathbb{R}^2 : -1 \le \tau \le 1, v_1(\tau) \le \sigma \le v_2(\tau)\},$$

and Equation (6) becomes

$$\sum_{\mu=1}^{Q} d_\mu \left[\psi_\mu(x,t) - \int_{-1}^{1} \int_{-1}^{1} \int_{v_1(\tau)}^{v_2(\tau)} \frac{t}{2} K(x,t,\sigma,\tau,s(t,\theta)) \psi_\mu(\sigma,\tau,s(t,\theta)) \, \mathrm{d}\sigma \, \mathrm{d}\tau \, \mathrm{d}\theta \right] = f(x,t). \tag{7}$$

Now the interval $[v_1(\tau), v_2(\tau)]$ is converted to the fixed interval $[-1, 1]$ by the following linear transformation:

$$\sigma(\tau, z) = \frac{v_2(\tau) - v_1(\tau)}{2} z + \frac{v_2(\tau) + v_1(\tau)}{2}.$$

So, Equation (7) will become

$$\sum_{\mu=1}^{Q} d_\mu \left[\psi_\mu(x,t) - \int_{-1}^{1} \int_{-1}^{1} \int_{-1}^{1} K_1(x,t,\sigma(\tau,z),\tau,s(t,\theta)) \psi_\mu(\sigma(\tau,z),\tau,s(t,\theta)) \, \mathrm{d}z \, \mathrm{d}\tau \, \mathrm{d}\theta \right] = f(x,t), \tag{8}$$

where

$$K_1(x,t,\sigma(\tau,z),\tau,s(t,\theta)) = \frac{t}{2} \frac{v_2(\tau) - v_1(\tau)}{2} K(x,t,\sigma(\tau,z),\tau,s(t,\theta)).$$

Assume that Equation (8) holds at the collocation points $(x_i, t_r), i = 0, \ldots, N, r = 0, \ldots, M$. So, we have

$$\sum_{\mu=1}^{Q} d_\mu \left[\psi_\mu(x_i,t_r) - \int_{-1}^{1} \int_{-1}^{1} \int_{-1}^{1} K_1(x_i,t_r,\sigma(\tau,z),\tau,s(t_r,\theta)) \psi_\mu(\sigma(\tau,z),\tau,s(t_r,\theta)) \, \mathrm{d}z \, \mathrm{d}\tau \, \mathrm{d}\theta \right] = f(x_i,t_r). \tag{9}$$

Using an m-point quadrature formula with the points $\{\theta_l\}, \{\tau_p\}, \{z_q\}$ in the interval $[-1, 1]$ and weights $\{w_l\}, \{w_p\}, \{w_q\}$ for numerical integration in Equation (9), we conclude

$$\sum_{\mu=1}^{Q} d_\mu \left[\psi_\mu(x_i,t_r) - \sum_{l=1}^{m} \sum_{p=1}^{m} \sum_{q=1}^{m} K_1(x_i,t_r,\sigma(\tau_p,z_q),\tau_p,s(t_r,\theta_l)) \psi_\mu(\sigma(\tau_p,z_q),\tau_p,s(t_r,\theta_l)) w_p w_q w_l \right] = f(x_i,t_r). \tag{10}$$

Solving Equation (10) using a method such as TSVD leads to the quantities d_μ, and then the values of $u(x,t)$ at any point of $\Omega \times [0,T]$ can be approximated by

$$u(x,t) \approx \sum_{\mu=1}^{Q} d_\mu \psi_\mu(x,t), \quad (x,t) \in \Omega \times [0,T].$$

In the case Ω is a domain of the third kind, we can write $\Omega = \Omega_1 \cup \Omega_2 \cup \cdots \cup \Omega_d$, where Ω_i, $1 \le i \le d$, are disjoint domains of the first or second kind. So, we have

$$\sum_{\mu=1}^{Q} d_\mu \left[\psi_\mu(x_i,t_r) - \sum_{e=1}^{d} \sum_{l=1}^{m} \sum_{p=1}^{m} \sum_{q=1}^{m} K_1(x_i,t_r,\sigma_e(\tau_p,z_q),\tau_p,s(t_r,\theta_l))\psi_\mu \right.$$
$$\left. (\sigma_e(\tau_p,z_q),\tau_p,s(t_r,\theta_l))w_p w_q w_l \right] = f(x_i,t_r), \tag{11}$$

where

$$\sigma_e(\tau,z) = \frac{v_{2,e}(\tau) - v_{1,e}(\tau)}{2} z + \frac{v_{2,e}(\tau) + v_{1,e}(\tau)}{2}. \tag{12}$$

As we mentioned, $v_{1,e}$ and $v_{2,e}$ are continuous functions relative to the sub-domain Ω_e.

We emphasize that this transformation is only considered for integration in (ξ, s) domain, and so the variables (x,t) are not changed, and the pseudospectral methods cannot be used.

4. Numerical examples

In this section, we present some numerical examples where Ω is a bounded domain in $\mathbb{R}^n$ ($n = 1, 2$). Due to the restrictions of the optimal choice for the shape parameter c, we have selected the parameter in all the examples experimentally. Tables 2–7 show the estimation of the parameter c for different values of M and N. It is shown that the maximum absolute errors are completely dependent on the values of M, N, and c. As the RBF shape parameter becomes smaller, corresponding to flat RBFs, the accuracy will be better, but the interpolation matrix becomes ill-conditioned. Also, we have used the five-point Gauss–Legendre quadrature rule for numerical integration. All calculations were supported by the Maple 13.

Example 1 (See [14]) Consider the equation

$$u(x,t) - \int_0^t \int_\Omega K(x,t,\xi,s)u(\xi,s)\,\mathrm{d}\xi\,\mathrm{d}s = f(x,t), \quad (x,t) \in \Omega \times [0,2],$$

with $\Omega = [0,2]$ and

$$K(x,t,\sigma,s) = -\cos(x-\sigma)\exp(-(t-s)),$$
$$f(x,t) = \exp(-t)(\cos(x) + t\cos(x) + \tfrac{1}{2}t\cos(x-2)\sin(2)).$$

The exact solution is $u(x,t) = \exp(-t)\cos(x)$. The absolute errors for different values of M and N and $c = 0.01$ are shown in Figure 1. Moreover, the maximum absolute errors for different values of M, N, and c are given in Table 2. From Figure 1 and Table 2, it can be seen that the present method very well coincides with the exact solution. In fact, as M and N increase and the shape

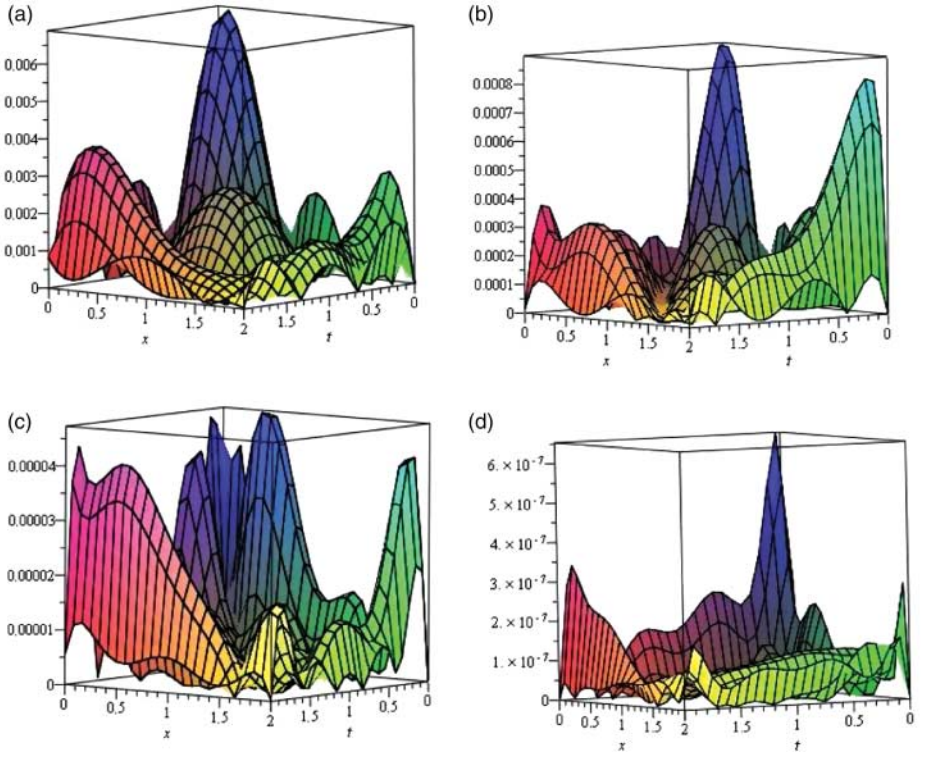

Figure 1. The absolute errors of Example 1 for $c = 0.01$. (a) $M = N = 3$, (b) $M = N = 4$, (c) $M = N = 5$, and (d) $M = N = 7$.

Table 2. Maximum absolute errors for different values of M, N, and c.

M, N	$c = 0.8$	$c = 0.1$	$c = 0.01$
3, 3	5.0×10^{-2}	7.0×10^{-3}	6.0×10^{-3}
5, 5	6.0×10^{-3}	2.0×10^{-4}	4.0×10^{-5}
7, 7	6.0×10^{-4}	5.0×10^{-6}	6.0×10^{-7}

parameter becomes smaller, the absolute errors decrease significantly and the results will rapidly tend to the exact values.

Example 2 Now consider the Volterra–Fredholm integral equation (1) which is defined on a non-rectangular domain Ω with

$$\Omega = \left\{(\sigma, \tau) \in \mathbb{R}^2 : 0 \le \sigma \le \frac{\pi}{4}, \sin(\sigma) \le \tau \le \cos(\sigma)\right\}, \quad T = 1,$$

and

$$K(x, y, t, \sigma, \tau, s) = 1 + \sin(x) + y,$$

with the exact solution $u(x, y, t) = x + t$, and define $f(x)$ accordingly. Figure 2 shows the absolute errors for various values of M, N, and $c = 0.001$ with $t = 0.5$. Also, the numerical results are presented in Table 3 in terms of maximum absolute errors at different values for M, N, and c.

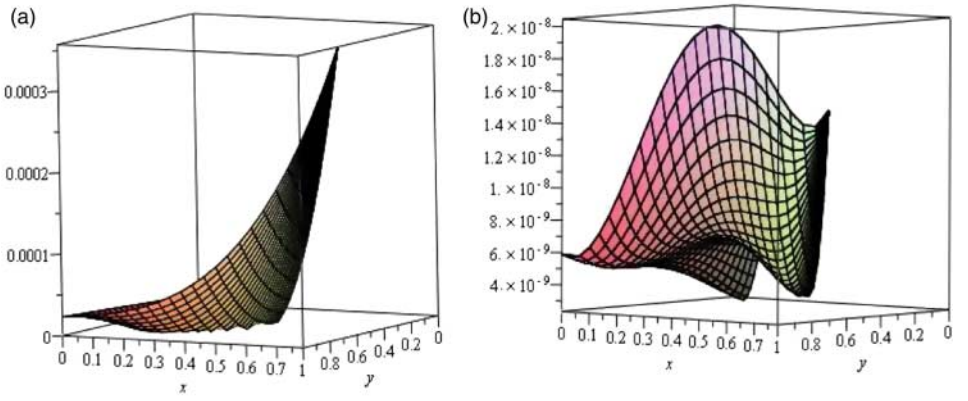

Figure 2. The absolute errors of Example 2 for $t = 0.5$ and $c = 0.001$. (a) $M = 2, N = 3$ and (b) $M = 3, N = 10$.

Table 3. Maximum absolute errors for different values of M, N, and c with $t = 0.5$.

M, N	$c = 0.2$	$c = 0.02$	$c = 0.001$
3, 3	6.0×10^{-2}	6.0×10^{-3}	3.0×10^{-4}
3, 10	7.0×10^{-4}	8.0×10^{-6}	2.0×10^{-8}

Table 3 is considered to illustrate the effect of M, N, and the shape parameter c on RBF solutions. This table shows that by increasing M and N and reducing c, the absolute errors decrease rapidly.

Example 3 In this example, we consider the Volterra–Fredholm integral equation (1), where

$$K(x, y, t, \sigma, \tau, s) = 1 + x + \sin(y),$$
$$f(x, y, t) = xt - \tfrac{7}{24}t^2 - \tfrac{7}{24}t^2 x - \tfrac{7}{24}t^2 \sin(y),$$

with the exact solution $u(x, y, t) = xt$. We consider the region Ω as follows:

$$\Omega = \{(\sigma, \tau) \in \mathbb{R}^2 : -1 \le \tau \le 1, v_1(\tau) \le \sigma \le v_1(\tau)\}, \quad T = 1,$$

where

$$v_1(\tau) = \begin{cases} 0, & -1 \le \tau \le 0, \\ -\sqrt{\tau - \tau^2}, & 0 \le \tau \le 1, \end{cases}$$

and

$$v_2(\tau) = \sqrt{1 - \tau^2}.$$

The traditional methods have some difficulties with regard to the numerical solution of this problem due to the irregularity of its domain. But using some nodes scattered over the Ω, this problem could be solved using the meshless method proposed in this paper. The graphs of the absolute errors are presented in Figure 3 for different values of M and N and $c = 0.001$ with $t = 0.5$, and the maximum absolute errors are given in Table 4.

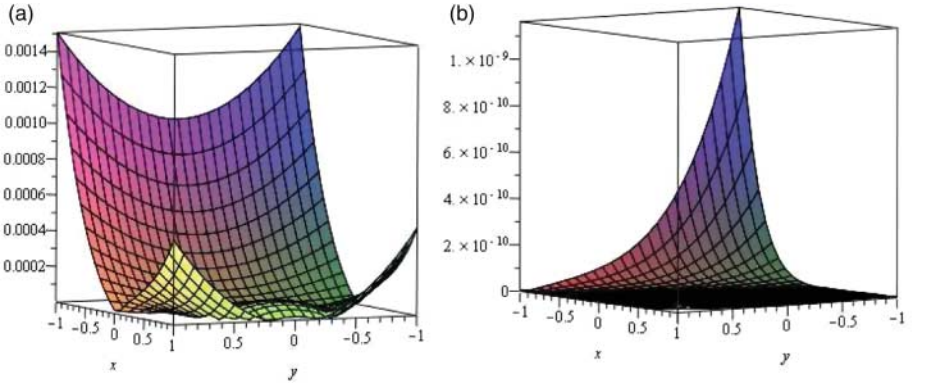

Figure 3. The absolute errors of Example 3 for $t = 0.5$ and $c = 0.001$. (a) $M = N = 4$ and (b) $M = 5, N = 34$.

Table 4. Maximum absolute errors for different values of M, N, and c for $t = 0.5$.

M, N	$c = 0.9$	$c = 0.1$	$c = 0.001$
3, 3	4.0×10^{-1}	1.2×10^{-1}	1.5×10^{-3}
4, 9	4.0×10^{-1}	8.0×10^{-2}	9.0×10^{-4}
4, 34	2.0×10^{-1}	1.4×10^{-3}	1.4×10^{-9}

Example 4 Consider the following mixed Volterra–Fredholm integral equation:

$$u(x,t) - \int_0^t \int_\Omega K(x,t,\xi,s)u(\xi,s)\,\mathrm{d}\xi\,\mathrm{d}s = f(x,t), \quad (x,t) \in \Omega \times [0,T],$$

where

$$K(x,y,t,\sigma,\tau,s) = t^2\cos(x),$$
$$f(x,y,t) = \sin(xt) - \tfrac{1}{2}t^2\cos(x) + \cos(x) - \cos(x)\cos(t),$$
$$\Omega = \{(\sigma,\tau) \in \mathbb{R}^2 : 0 \le \sigma \le 1, \sigma^2 \le \tau \le \sigma\}, \quad T = 1.$$

The exact solution of this equation is $u(x,y,t) = \sin(xt)$.

Figure 4 shows the absolute errors for the RBF collocation method for different values of M and N and $c = 0.001$ with $t = 0.5$, and the maximum absolute errors are reported in Table 5.

Example 5 In this example, we consider the mixed Volterra–Fredholm integral equation

$$u(x,y,t) - \int_0^t \int_\Omega s\sigma^2 \exp(5\mathrm{i}\sigma)u(\sigma,\tau,s)\,\mathrm{d}\sigma\,\mathrm{d}\tau\,\mathrm{d}s = f(x,y,t), \quad (x,y,t) \in \Omega \times [0,1],$$

where $\Omega = [0,1] \times [0,1]$ and define $f(x,y,t)$ accordingly. The exact solution of this equation is $u(x,y,t) = x\cos(y)$ and the kernel is oscillatory kernel. For this example, we have used the following regular points:

$$\left\{ \left(\frac{i}{n-1}, \frac{j}{n-1} \right) \middle| \, 0 \le i,j \le n-1 \right\},$$

and Halton points which are random points in Ω [6]. Tables 6 and 7 show the maximum absolute errors for different values of M, N, and c for regular points and Halton points. Also, the absolute errors are shown in Figure 5 for $M = 3, N = 15$ at $y = 0.4$ and $c = 0.1$.

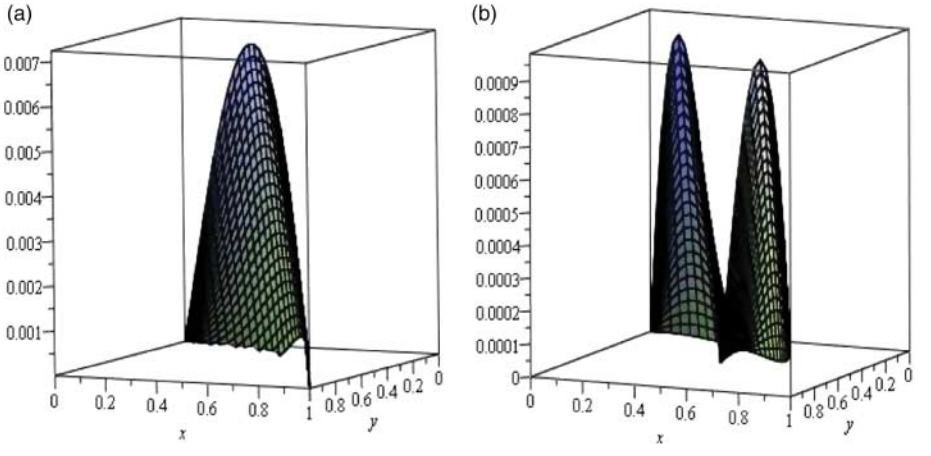

Figure 4. The absolute errors for Example 4 for $t = 0.5$ and $c = 0.001$. (a) $M = N = 2$ and (b) $M = 3, N = 5$.

Table 5. Maximum absolute errors for different values of M, N, and c for $t = 0.5$.

M, N	$c = 1.5$	$c = 0.1$	$c = 0.001$
2, 2	9.0×10^{-2}	3.0×10^{-2}	7.0×10^{-3}
5, 5	2.0×10^{-2}	1.8×10^{-3}	9.0×10^{-4}

Table 6. Maximum absolute errors for different values of M and N with $c = 0.1$.

	Halton points		Regular points	
y	$M = N = 3$	$M = 3,\ N = 15$	$M = N = 3$	$M = 3,\ N = 15$
0	6.0×10^{-2}	7.0×10^{-4}	1.0×10^{-2}	1.0×10^{-4}
0.2	3.0×10^{-2}	3.0×10^{-4}	5.0×10^{-2}	8.0×10^{-4}
0.4	1.0×10^{-2}	1.8×10^{-4}	8.0×10^{-2}	1.0×10^{-4}
0.6	3.0×10^{-2}	1.6×10^{-4}	8.0×10^{-2}	9.0×10^{-4}
0.8	1.0×10^{-1}	1.4×10^{-4}	5.0×10^{-2}	5.0×10^{-4}
1.0	2.0×10^{-1}	1.0×10^{-3}	1.0×10^{-2}	5.0×10^{-4}

Table 7. Maximum absolute errors for different values of M and N with $c = 0.8$.

	Halton points		Regular points	
y	$M = N = 3$	$M = 3,\ N = 15$	$M = N = 3$	$M = 3,\ N = 15$
0	1.0×10^{-1}	2.0×10^{-2}	8.0×10^{-2}	1×10^{-3}
0.2	1.2×10^{-1}	8.0×10^{-3}	9.0×10^{-2}	8×10^{-3}
0.4	1.4×10^{-1}	4.0×10^{-3}	8.0×10^{-2}	1×10^{-3}
0.6	1.6×10^{-1}	6.0×10^{-3}	6.0×10^{-2}	9×10^{-3}
0.8	1.4×10^{-1}	5.0×10^{-3}	4.0×10^{-2}	5×10^{-3}
1.0	1.0×10^{-1}	5.0×10^{-3}	4.0×10^{-2}	5×10^{-3}

As it is seen in Tables 6 and 7, since the Halton points are uniformly distributed in Ω, there is no significant differences between the use of these points and the regular points.

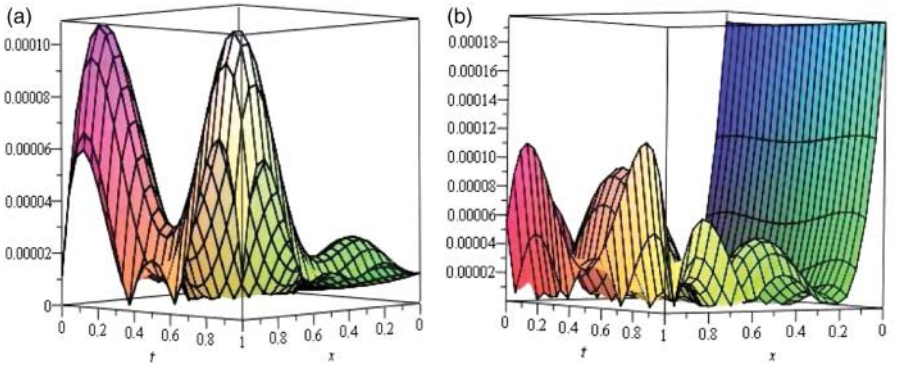

Figure 5. The absolute errors for Example 5 with $M = 3$, $N = 15$ at $y = 0.4$ for $c = 0.1$. (a) Regular points and (b) Halton points.

5. Conclusion

In this paper, a collocation method based on RBFs for numerical solution of mixed Volterra–Fredholm integral equations is presented. The proposed method is a meshless method which needs only a scattered set of nodes in the domain instead of a mesh. Also, the geometry of the domain does not play an important role in the presented method. These are significant advantages of the method.

References

[1] E. Banifatemi, M. Razzaghi, and S. Yousefi, *Two-dimensional Legendre wavelets method for the mixed Volterra–Fredholm integral equations*, J. Vib. Control 13 (2007), pp. 1667–1675.
[2] T. Belytschko, Y.Y. Lu, and L. Gu, *Element-free Galerkin methods*, Int. J. Numer. Methods Eng. 37 (1994), pp. 229–256.
[3] H. Brunner, *On the numerical solution of nonlinear Volterra–Fredholm integral equations by collocation methods*, SIAM J. Numer. Anal. 27(4) (1990), pp. 987–1000.
[4] H. Brunner, *Collocation Methods for Volterra Integral and Related Functional Equations*, Cambridge University Press, Cambridge, 2004.
[5] O. Diekman, *Thresholds and traveling waves for the geographical spread of infection*, J. Math. Biol. 6 (1978), pp. 109–130.
[6] G.E. Fasshauer, *Meshfree Approximation Methods with Matlab*, World Scientific Publishing, Singapore, 2007.
[7] G.E. Fasshauer and J.G. Zhang, *On choosing optimal shape parameters for RBF approximation*, Numer. Algorithms 45 (2007), pp. 346–368.
[8] B. Fornberg and C. Piret, *On choosing a radial basis function and a shape parameter when solving a convective PDE on a sphere*, J. Comput. Phys. 227 (2008), pp. 2758–2780.
[9] H. Guoqiang, *Asymptotic error expansion for the Nystrom method for a nonlinear Volterra–Fredholm integral equations*, J. Comput. Appl. Math. 59 (1995), pp. 49–59.
[10] H. Guoqiang and Z. Liqing, *Asymptotic expansion for the trapezoidal Nystrom method of linear Volterra–Fredholm equations*, J. Comput. Appl. Math. 51(3) (1994), pp. 339–348.
[11] L. Hacia, *On approximate solution for integral equations of mixed type*, ZAMM Z. Angew. Math. Mech. 76 (1996), pp. 415–416.
[12] R.L. Hardy, *Multiquadric equations of topography and other irregular surfaces*, J. Geophys. Res. 76 (1971), pp. 1905–1915.
[13] P.J. Kauthen, *Continuous time collocation methods for Volterra–Fredholm integral equations*, Numer. Math. 56 (1989), pp. 409–424.
[14] K. Maleknejad and M. Hadizadeh, *A new computational method for Volterra–Fredholm integral equations*, Comput. Math. Appl. 37 (1999), pp. 1–8.
[15] Y.X. Mukherjee and S. Mukherjee, *The boundary node method for potential problems*, Int. J. Numer. Methods Eng. 40 (1997), pp. 797–815.
[16] B.G. Pachpatte, *On mixed Volterra–Fredholm type integral equations*, Indian J. Pure Appl. Math. 17 (1986), pp. 488–496.

[17] S. Rippa, *An algorithm for selecting a good value for the parameter c in radial basis function interpolation*, Adv. Comput. Math. 11 (1999), pp. 193–210.
[18] I.J. Schoenberg, *Metric spaces and completely monotone functions*, Ann. Math. 39 (1938), pp. 811–841.
[19] H.R. Thieme, *A model for the spatio spread of an epidemic*, J. Math. Biol. 4 (1977), pp. 337–351.
[20] A.M. Wazwaz, *A reliable treatment for mixed Volterra–Fredholm integral equations*, Appl. Math. Comput. 127 (2002), pp. 405–414.
[21] A. Yildirim, *Homotopy perturbation method for the mixed Volterra–Fredholm integral equations*, Chaos Solitons Fractals 2 (2009), pp. 2760–2764.
[22] C. Zuppa, *Error estimates for moving least square approximations*, Bull. Braz. Math. Soc. New Series 34(2) (2003), pp. 231–249.